Hindawi Publishing Corporation
Advances in Condensed Matter Physics
Volume 2012, Article ID 364376, 8 pages
doi:10.1155/2012/364376

Research Article

Bipolar Resistive Switching Characteristic of Epitaxial NiO Thin Film on Nb-Doped $SrTiO_3$ Substrate

Yongdan Zhu[1,2] and Meiya Li[1]

[1] *School of Physics and Technology and Key Laboratory of Artificial Micro/Nano Structures of the Ministry of Education, Wuhan University, Wuhan 430072, China*
[2] *School of Information Engineering, Hubei University for Nationalities, Enshi, Hubei 445000, China*

Correspondence should be addressed to Meiya Li, myli@whu.edu.cn

Received 22 May 2012; Accepted 31 July 2012

Academic Editor: A. Alexandrov

Epitaxial NiO film was grown on 0.7% Nb-doped $SrTiO_3$ substrates by pulsed laser deposition. The I-V characteristics of Ag/NiO/Nb-$SrTiO_3$/In device show reproducible and pronounced bipolar resistive switching without forming process which was induced by the NiO/Nb-$SrTiO_3$ junctions, and the resistive switching ratio R_{HRS}/R_{LRS} can reach 10^3 at the read voltage of -0.5 V. Furthermore, the resistance states can be controlled by changing the max forward voltage, reverse voltage, or compliance current, indicating multilevel memories. These results were discussed by considering the role of carrier injection trapped/detrapped at the interfacial depletion region of the heterojunction.

1. Introduction

Recently, the resistance switching (RS) effect has attracted a great deal of scientific and technological interests due to the potential applications in the resistance random access memory (RRAM). Among other nonvolatile random memories, RRAM has excellent advantages such as high cell density, high operation speed, low power consumption, low cost, and good endurance [1, 2]. RS effect has been observed in many oxide systems include binary metal oxides NiO, TiO_2, ZrO_2, ZnO and complex perovskite oxides $Pr_{0.7}Ca_{0.3}MnO_3$, and $SrTiO_3$, variety of material crystalline, from single crystal, epitaxial films to polycrystalline; different device structures from sandwiches to heterostructure junctions [3–21]. NiO is one of these materials which have been observed unipolar or bipolar RS effect. Kawai et al. studied the bipolar RS switching in epitaxial NiO films-based Pt/NiO/Pt : Ir device on MgO substrate [4]. Choi et al. compared RS of NiO films deposited on Pt and $SrRuO_3$ which has unipolar switching in Pt/NiO/Pt and bipolar switching in Pt/NiO/$SrRuO_3$ [5]. Chang et al. observed two types of reversible RS effects in a NiO film: memory RS at low temperature and threshold RS at high temperature [7]. To explain the interesting effect, many theoretical models have been proposed, in which the most basic mechanisms are electrochemical redox process and Schottky-like barrier by trapped/detrapped effects at interface. Moreover, recent molecular dynamic simulations of memristors were reported by Savel'ev et al. for understanding the RS mechanism in depth [22–24]. However, despite its fundamental importance, our understanding of the underlying RS physics is still an open question because of the different preparing method and equipment [25].

Band insulating perovskite $SrTiO_3$ is widely used substrate materials in oxide device preparations. In $SrTiO_3$, substitution of Ti^{+4} by Nb^{+5} leads to Nb-doped STO (NSTO), which is as electron-doped oxide semiconductors with low resistance. By using PLD technique, other conducting oxide layers such as $SrRuO_3$ (SRO) and doped CMR manganites of PCMO can be epitaxial growth on n-type oxide semiconductor substrates of NSTO to fabricate oxide heterostructure junctions [20, 21]. Rectifying curves were observed in heterostructure devices of $SrRuO_3$/NSTO, $PrCaMnO_3$/NSTO and metal electrode/NSTO that demonstrated forming bias barriers by mobile carriers at interfaces as oxide hetero-junctions. Recently, Sullaphen et al. reported the RS properties of epitaxial NiO nanostructures on NSTO substrates. The switching behavior (dependence on height) is attributed to the modulation of the carrier density at the

nanostructure-substrate interface due to the applied electric field [10]. NiO is one of the typical *p*-type semiconductors which are induced by Ni vacancy, and there are many RS effect researches on NiO based device. It must be pointed out that the interface can be better controlled and the epitaxial films can be realized, which is helpful for understanding the mechanisms of RS effect. So it is very important to study the RS effect in heterojunction between NiO and NSTO.

2. Experiment

Epitaxial NiO thin film was grown on the 0.7% Nb-doped $SrTiO_3$ (100) single crystal substrate by pulsed laser deposition (PLD) technique using a KrF excimer laser ($\lambda = 248$ nm). The substrate temperature was kept at 650°C, the oxygen pressure of 20 Pa was maintained throughout the deposition, and the ceramic NiO target was used. After growth, the crystalline structure of the film was characterized by Bruker D8 Advance X-ray diffractometer with Cu Kα radiation. The thickness of the NiO film was about 80 nm determined by Form Talysurf Profiler (S4C-3D, Taylor Hobson). XPS was performed by VG Multilab 2000 instrument and all XPS spectra were calibrated by the C1s peak 284.6 eV from contamination to compensate the charge effect. Before the electrical measurements, Ag electrodes were deposited on the thin film using DC magnetron sputtering through a shadow mask with a diameter of 0.2 mm and the bottom electrode In was pressed on the NSTO to form ohmic contacts. *I-V* characteristics of the Ag/NiO/NSTO/In device were measured with two-probe configuration by Keithley-4200SCS. The current from NiO to NSTO was defined as a positive direction. RS effect of the junctions was investigated by applying bias at room temperature.

3. Results and Discussion

Figure 1(a) shows the XRD pattern of NiO film deposited on NSTO. As can be seen from the θ-2θ pattern in Figure 1(a), the NiO film exhibits only (200) orientation without any other diffraction peaks, suggesting (200) orientation growth of the film. XRD Φ-scan has been carried out to identify the epitaxial growth of the (200) oriented NiO film on NSTO. Figure 1(b) shows the Φ-scan patterns of the film along (111) planes with four peaks located at every 90° in the pattern, indicating the epitaxial growth of NiO on NSTO (100) substrate. A rocking curve of NiO(200) with a full width at half maximum of 1.58° was shown in Figure 1(c), indicating the good quality of the epitaxial film. The lattice constant of NiO in out of plane direction calculated from the XRD pattern is 4.20 Å. Since the lattice constant of bulk NiO is 4.177 Å and NSTO is 3.905 Å, a lattice mismatch of 7.0% existed between them. Therefore, the NiO film would receive an in-plane compressive strain from the substrate and result in a lattice extension in out-of-plane direction. Similar results were also reported in NiO epitaxial films [4–6].

To analyze the chemical states of the constituent elements, XPS measurement was performed. Figure 1(d) shows the typical Ni2p XPS spectrum of the NiO film. The binding energy of Ni 2p3/2 is located at about 854.3 eV in the spectrum, consistent well with that expected by theory for Ni^{2+} (854.3 eV) within a certain range of error, indicating Ni^{2+} ions are dominant in this sample. Figure 1(e) presents the O1s XPS spectrum of the NiO film and the large peak is well fitted by two nearly Gaussian components, centered at 529.7 eV (O_a) and 531.75 eV (O_b), respectively. The O_a peak at a low binding energy is attributed to the Ni-O bonds [26],while the O_b peak at higher binding energy is usually attributed to the chemisorbed or dissociated oxygen or OH species on the surface of the NiO film, such as $-CO_3$, adsorbed H_2O or O_2. Therefore, the large and high O_a peak suggests that the Ni-O bonds are the main chemical state in the NiO film.

The current-voltage (*I-V*) characteristic of the Ag/NiO/NSTO/In device has been measured at different sweep voltage or compliance current with the sequence of $0V \rightarrow V_{max} \rightarrow 0 \rightarrow -V_{max} \rightarrow 0$. Figure 2(a) shows the typical stable bipolar RS behavior's *I-V* data under ±5 V sweep voltage for many cycles without forming process, and the heterojunction exhibits a rectifying behavior and remarkable hysteresis under forward or reverse bias. The resistance of the device switched from the HRS to LRS by applying a positive voltage and then recovered to HRS by applying a negative voltage. The R_{HRS}/R_{LRS} ratio read at −0.5 V has been obtained about larger than 10^3. As can be seen, there is no degradation between the first cycle and 100 cycles, indicating good endurance. The large RS and good endurance make this device suitable for memory application. The RS ratio was defined as R_{HRS}/R_{LRS}, which was shown in Figure 2(b). We can see that, at the low read voltage, the RS ratio can reach a large value, but decrease with the increasing read voltages. So the low read voltage is a great advantage in our device.

The RS effect can be obtained at the ±5 V sweep voltage and 0.1A compliance current. In order to investigate the origin of bipolar RS effect, the effect of different forward or reverse voltage and compliance current should be studied in detail. The enough reverse voltage can drive the RS to HRS, and the forward bias can force the resistance state to LRS; when the reverse voltage is defined −5 V, the influence of the forward voltage on LRS is very important. Figure 3(a) shows the *I-V* with the sequence of $0V \rightarrow +V_{max} \rightarrow 0 \rightarrow -5V \rightarrow 0$ with different $+V_{max}$; it must be emphasized that when the new sweep cycle started, the resistance state was switched to HRS by applying −5 V reverse voltage. As the forward voltage increases, the switching hysteresis in reverse voltage region becomes more and more pronounced the forward voltage dependence of the HRS and LRS; also shown in Figure 3(b). Accordingly, the RS ratio read at −0.5 V increases from 2 ($V_{max} = 1$ V) to 10^3 ($V_{max} > 3$ V), and when the forward voltage larger than 3 V, the ratio changes slightly. We also noticed that when increasing the forward voltage to 3 V, the sweep current went to a maximum value around −2.5 V and then decreased gradually up to −5 V. It shows a negative differential resistance occurring during the sweeping up to −5 V, which is a sufficient condition for bipolar resistive switching. This bias-induced bipolar RS

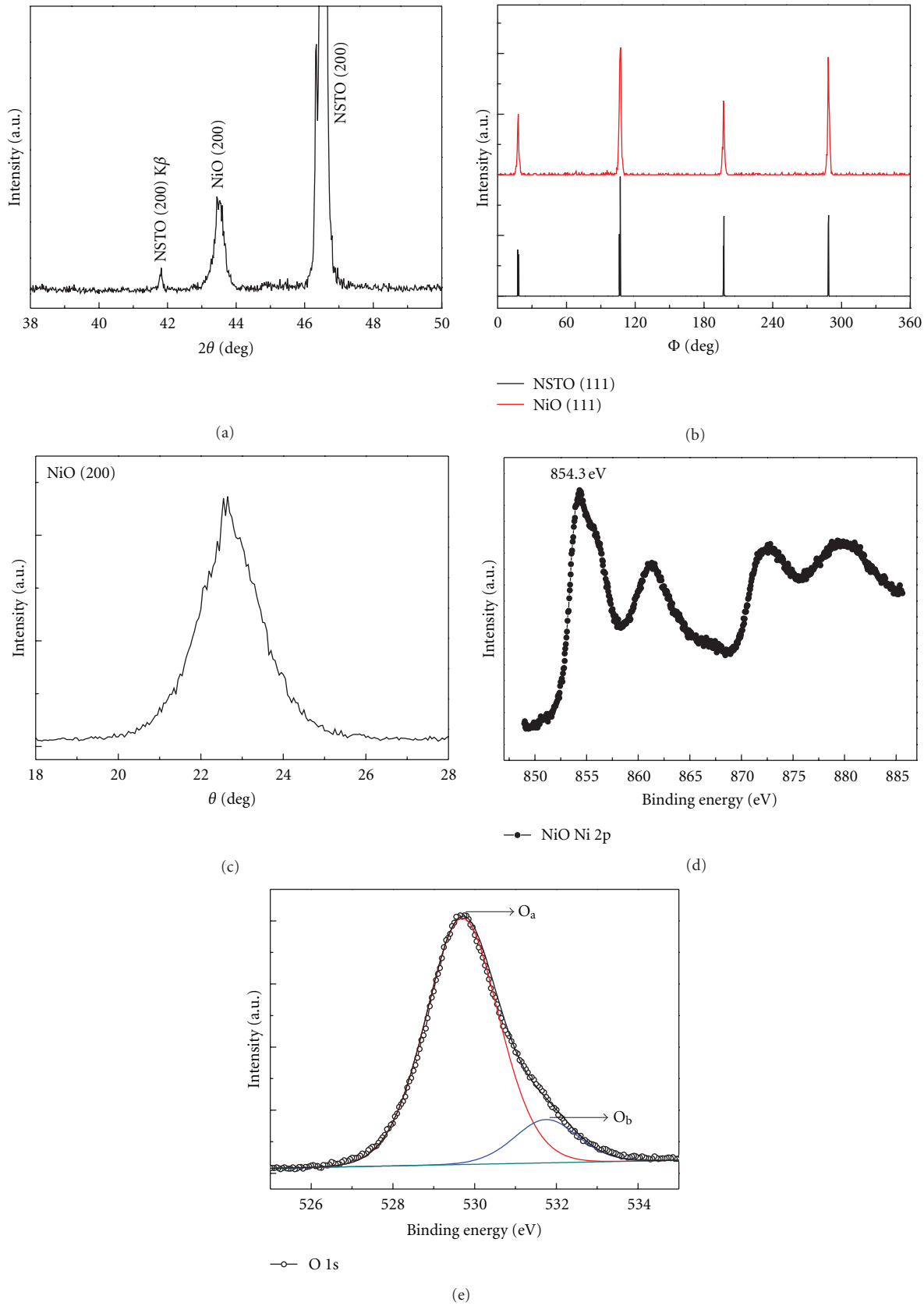

Figure 1: The XRD patterns for NiO/NSTO in θ-2θ scan (a) and Φ-scans of NiO (111) and NSTO (111) planes (b). Rocking curve scans of 200 peak for NiO (c). Typical XPS spectra of the NiO film for Ni 2p (d) and O1s (e).

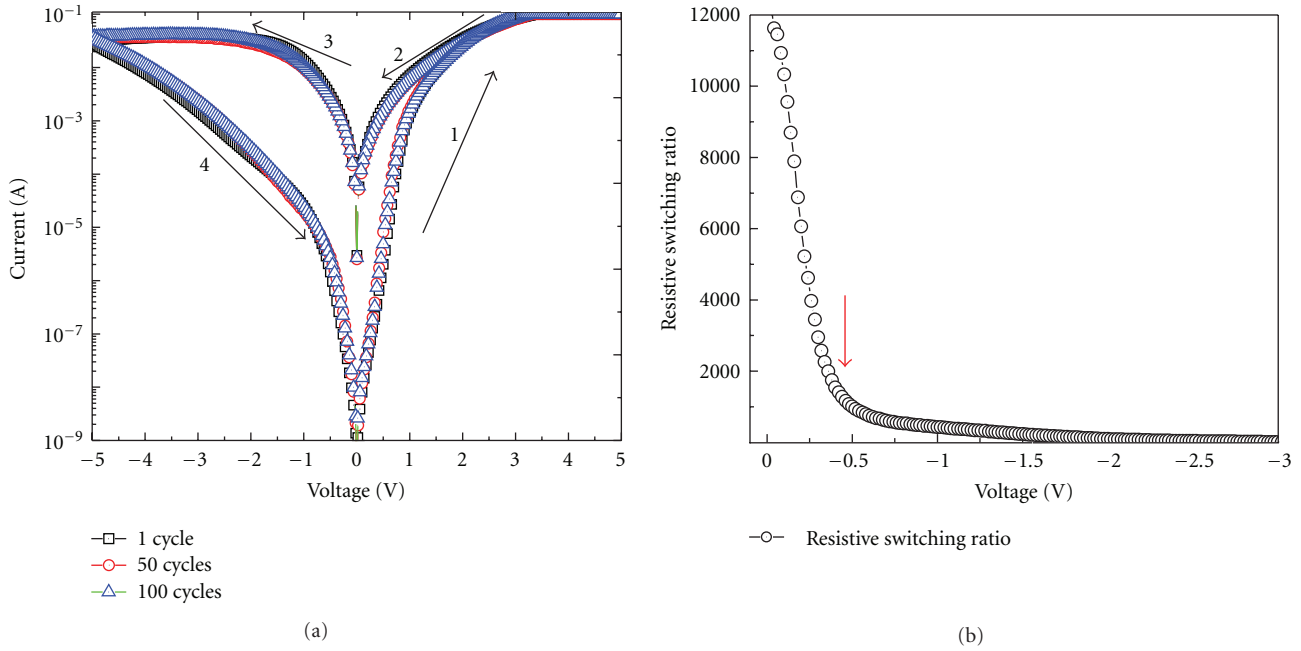

Figure 2: (a) Typical bipolar RS characteristics of Ag/NiO/NSTO/In device for the 1, 50, and 100 DC sweeping cycles. (b) The RS ratio dependence of the read voltages.

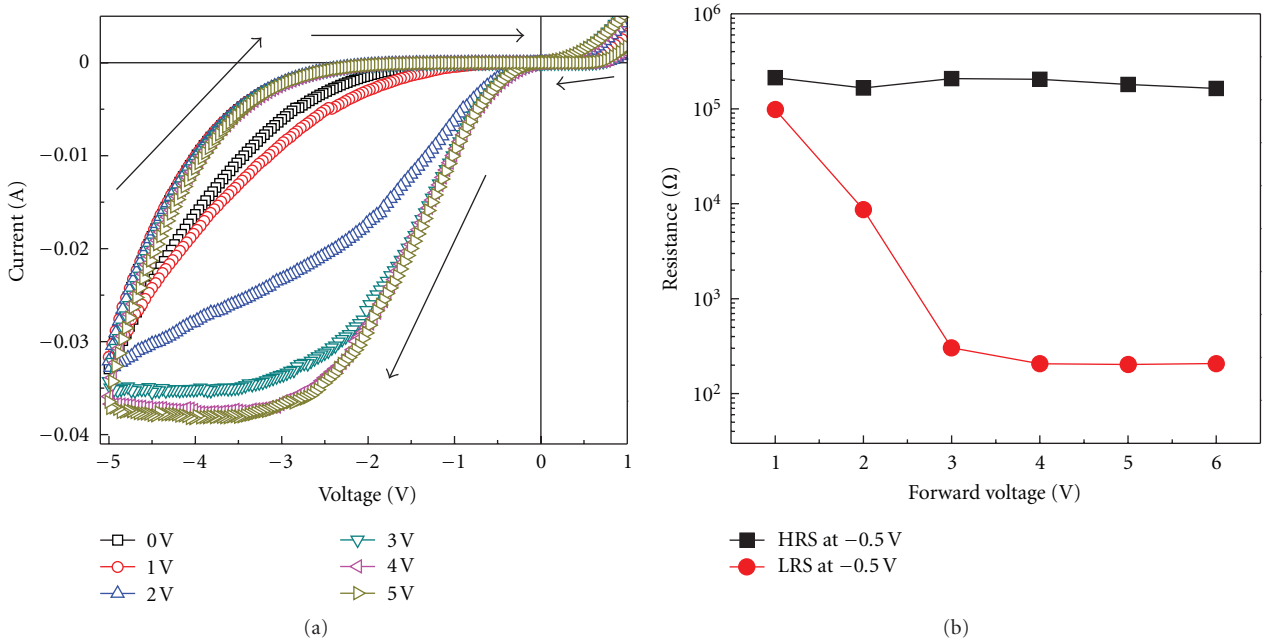

Figure 3: (a) The RS behavior after applying different forward voltage from 1 V to 6 V. (b) The forward voltage dependence of R_{HRS} and R_{LRS}.

effect was reported by Wu et al. in Pt/TiO_2/NSTO/Pt device and Pt/$LaAlO_3$/NSTO heterojunction [11, 12].

By changing the compliance current, a group of RS *I-V* curves under various set current compliances are measured are shown in Figure 4(a), at the reverse voltage region, the resistance states especially the LRS change by the compliance current, correspondingly, the rectifying behavior of LRS is also weakened. We can see that the LRS increases with the decreased compliance current. The compliance current dependence of the HRS and LRS are also shown

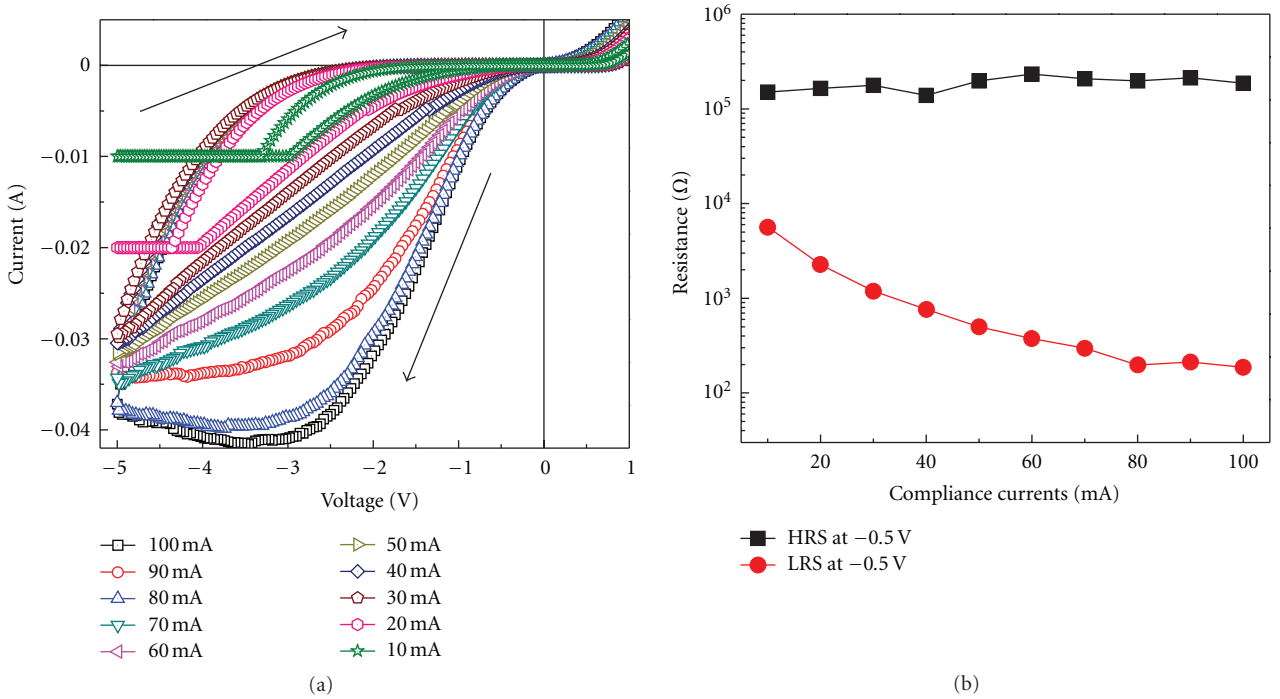

FIGURE 4: (a) RS characteristics for various compliance currents. (b) The compliance currents dependence of R_{HRS} and R_{LRS}.

in Figure 4(b) the R_{HRS}/R_{LRS} ratio measured at −0.5 V decreases from 10 (current compliance = 10 mA) to 10^3 (current compliance = 100 mA). So we can suggest that the NiO/NSTO device could realize multilevel memory storage by changing compliance current. Similar results were reported by Chen et al. by changing the compliance currents, the Fe_2O_3/NSTO can obtain multilevel memory [27].

The forward voltage or compliance current has influence on the RS which can change the LRS; the reverse voltage can drive the resistance state to HRS, so the reverse voltage magnitude could affect the HRS of the device. According to these views, a group of RS curves with various reverse voltages has been obtained as shown in Figure 5(a). It must be also emphasized that in the sweep cycle with a sequence of 0V → +5V → 0 → $-V_{max}$ → 0, when a new cycle started, the resistance state had been switched to the same LRS by applying +5 V forward voltage. As can be seen from Figure 5(a), the reverse voltage with large amplitude leads to large R_{HRS}; the R_{HRS} and R_{LRS} read at −0.5 V are shown in Figure 5(b), the R_{LRS} changes slightly because of the same forward voltage 5 V, but the R_{HRS} increases from $10^2\,\Omega$ (reverse voltage = 1 V) to $10^6\,\Omega$ (reverse voltage = −7 V) accordingly, the R_{HRS}/R_{LRS} ratio changes with the various reverse voltages. So we can also make a conclusion that the multilevel memory can be achieved by changing the reverse voltages. In addition, all the *I-V* curves except the curves with −1 V and −2 V show negative differential resistance occurring during the sweeping; only when the current reached the maximum value, the large R_{HRS}/R_{LRS} ratio could be obtained.

Wu et al. reported the reverse bias-induced bipolar RS in Pt/TiO_2/Nb : $SrTiO_3$/Pt devices which showed extremely weak RS hysteresis without applying reverse bias. But the reverse bias increased above −2 V and the hysteresis became more and more prominent. Based on their results, they suggested that there is a close relationship between RS and the modulation of Schottky-like barrier width by electrochemical migration of oxygen. And they also reported the $LaAlO_3$/Nb : $SrTiO_3$ bipolar RS device which can be explained by considering the migration of vacancies at the Pt/$LaAlO_3$ interface [11, 12]. Zhang et al. investigated the ultrafast RS effect of the Nb : STO with Ag and Pt, which is related to the barrier height of the junction [28]. Ni et al. reported the RS effect of $SrTiO_3$/Nb : STO heterojunction, and the RS effects were explained by considering the role of defects at the interface of the junction [17]. Sullaphen et al. reported the interface-mediated RS in epitaxial NiO nanostructures on NSTO. The overall switching behavior in NiO/NSTO heterojunction can be explained on the basis of field-induced modulation of the interface due to migration of minority charge carriers [10]. Although various models such as Schottky barrier with interface and electrochemical migration have been discussed to explain the RS effect, the origin of RS is still puzzled, because these models cannot explain all the RS results.

In order to investigate the switching mechanism for our device, the fitting of the *I-V* curves with various electrical conduction mechanisms was attempted. It was found that the conduction mechanism of LRS and HRS fits well to the space-charge-limited conduction (SCLC) mechanism. Other conduction mechanisms such as Schottky, Poole-Frenkel, and Fowler-Nordheim were investigated but they did not fit the *I-V* curves at all [17, 19]. Figure 6 shows the log-log plots for the *I-V* curve of NiO/NSTO. For the positive voltage

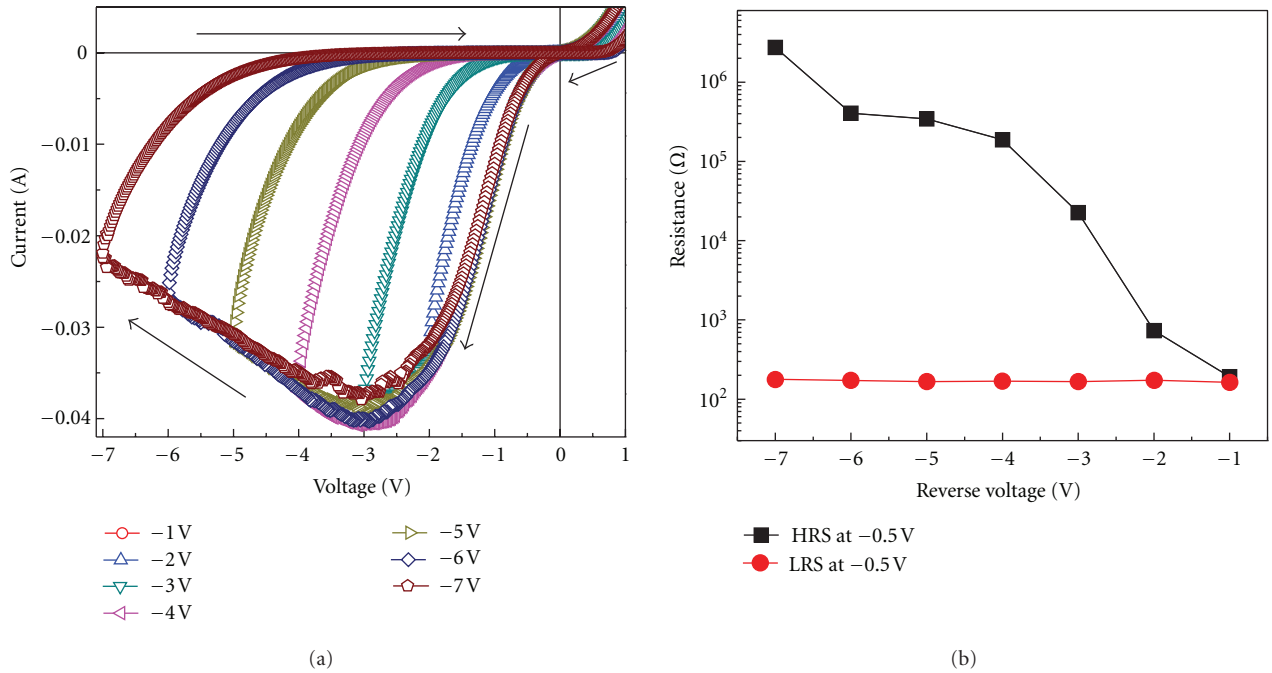

FIGURE 5: (a) The RS behavior after applying different reverse voltage from −1 V to −7 V. (b) The reverse voltage dependence of R_{HRS} and R_{LRS}.

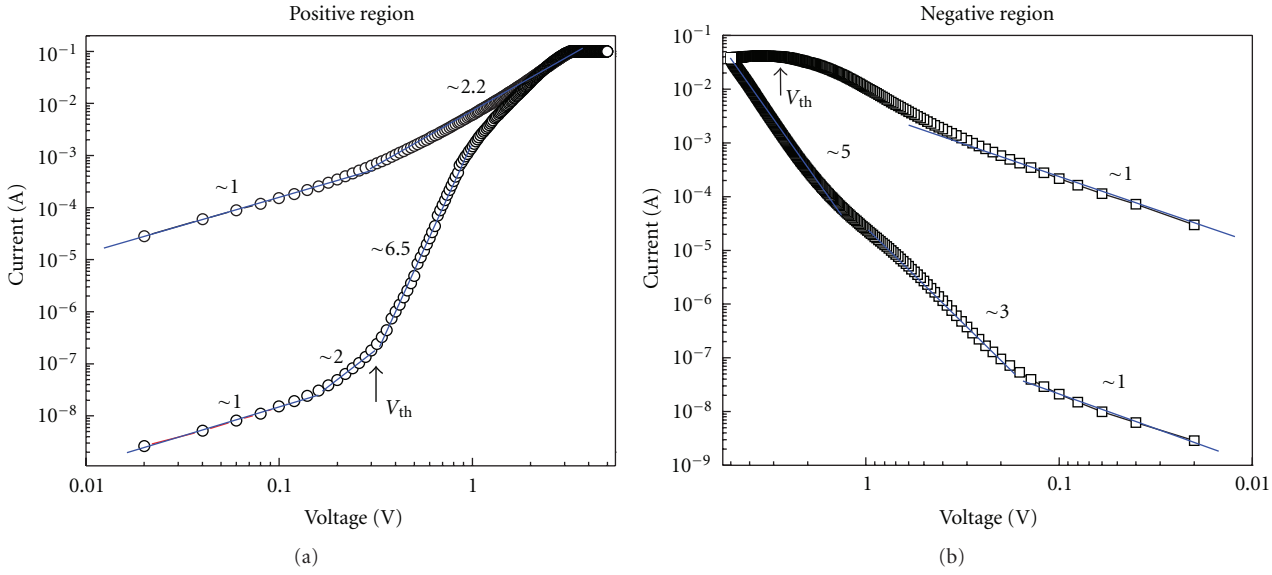

FIGURE 6: (Color online) *I-V* characteristics of switching memory cell in (a) positive bias region and (b) negative bias regions plotted in log-log scale.

region as shown in Figure 6(a), the *I-V* curve shows a linear behavior for $V < 0.2$ V, then a sharp current rise with a slope of 6.5 for $V > 0.3$ V (V_{th}) followed and finally increases slowly with slope of 2-3. This behavior can be well described by the trap controlled space-charge-limited current (SCLC mechanism) with the three regions corresponding to the trap-unfilled, trap-filled SCLC, and trap-free SCLC regimes, respectively. Moreover, V_{th} is the transition voltage from trap-unfilled to trap-filled SCLC regimes. Upon decreasing the voltage, the current remains the higher value indicating that the trapped carriers are not released from the trap centers, which result in the hysteresis of *I-V* curves. The reverse bias voltage (Figure 6(b)) releases the trapped carriers from the traps, leading to switch to the HRS.

As we know, NiO is a typical *p*-type semiconductor and the NSTO is *n*-type, and when epitaxial NiO was grown on NSTO substrate, the *p-n* junction with barrier can be formed at the interface. In this Ag/NiO/NSTO/In structure,

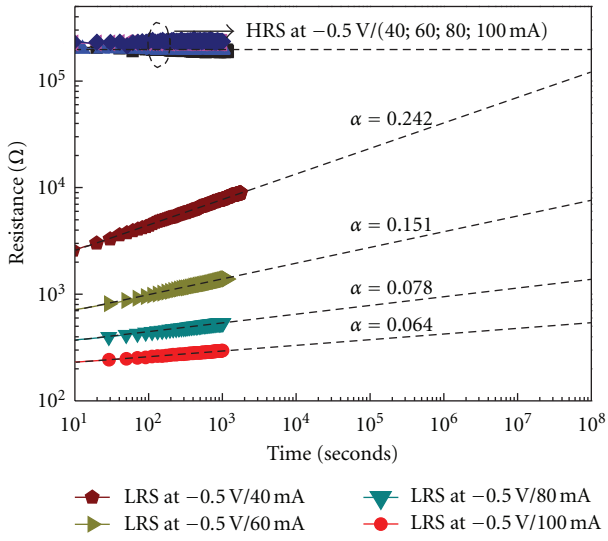

Figure 7: Resistance relaxation of the NiO/NSTO heterojunction with time after switching to LRSs and HRSs by +5 V or −5 V with different compliance current.

the RS behavior could be coming from following parts: the Ag/NiO, NiO/NSTO, NSTO/In interface. In order to estimate the contribution from Ag/NiO interface, the NiO film was deposited on insulated $SrTiO_3$ substrate and Ag was used as two top electrodes. It was shown that the *I-V* relationship of Ag/NiO/Ag was linear, indicating the ohmic contact between Ag and NiO. This is different from the RS behaviors of the Ag/NiO interface reported by Lee et al. [8] and Phark et al. [9]. We also prepared NiO film on Pt/Ti/SiO_2/Si substrate under the same preparation condition and formed Ag/NiO/Pt and Pt/NiO/Pt structure, and there is no RS effect observed in these structures. In addition, the Pt/NiO/NSTO/In was prepared and the RS effect was comparable with Ag/NiO/NSTO device, indicating the ohmic behavior of the NSTO/In interface. Furthermore, In was commonly used as electrode with ohmic contact for *I-V* measurement [19]. Therefore, the rectifying characteristic and RS effect in Ag/NiO/NSTO/In device are dominated by the NiO/NSTO interface. And some Ni vacancies and defects are distributed and relatively high near the interface which can form an active and positively charged trapping layer to trap electrons. So the characteristic of the junction is determined by the depletion layer. As from the above experimental results, the RS behavior could be explained by the consideration of the carrier injection trapped/detrapped at the interface of the heterojunction. When the forward voltage was applied on the device, the electric field mainly applied on the depletion layer. With carrier injection to the depletion layer, the build-in potential of the junction was weakened, consequently, the barrier width dramatically narrowed, and there by the electrons possibly pass through the thin barrier via a tunneling process, which corresponds to low resistance state. But the trapped electric cannot be released until a mount of reverse voltage is applied on the device. When the reverse voltage is applied on the device, the trapped carrier could be released, and the depletion barrier width could be widen and the depletion barrier height enhanced, so the enough reverse voltage results in HRS. Furthermore, the trapping centers could be filled by injected carriers, which can be controlled by applying electric field. Therefore, the resistance states can be controlled by changing the max forward voltage, reverse voltage, or compliance current, indicating multilevel memories, as shown in Figures 3–5.

Additionally, the original resistance of NiO films is about $10^6\ \Omega$, but the effective resistance of the LRS is much lower than the original resistance of NiO, so it is clearly demonstrated that the tunneling carriers are staying in the NiO films as to affect the resistance. That is, when the voltage is applied on the device, the device resistance consists of the interface of the heterojunction and the NiO films were switched, which lead to HRS and LRS. The whole device resistance can be modeled as a barrier diode and variable resistor. Our and other group's results display asymmetric RS effect at the forward and reverse voltage. The asymmetric RS effect can be explained based on our model [20, 21].

Generally speaking, the retention characteristic of heterojunction type RS device is not very stable. Ni et al. [17] have shown for $SrTiO_{3-x}$/NSTO heterojunction that the junction current relaxes with time after switching to the LRS and the relaxation follows the Curie-von Schweidler law at room temperature, indicating the role of defects in the interfacial depletion region. For understanding the mechanism of the RS effect and the types of defects in NiO/NSTO heterojunction, the relaxation of the junction current after switching to the LRS or HRS has been measured and the results are shown in Figure 7 in log-log scale. Each resistance state was driven by ±5 V voltage at different compliance currents. As shown in Figure 7, different compliance current can control the LRS of the NiO/NSTO device and the HRSs are at the same states. We can see that the HRSs are very stable, but the resistance relaxations of LRSs are different which follow liner behavior in the log-log scale. In other words, the resistance follows the law with $R = R_0 t^{-\alpha}$, where α is the slope which is a constant and less than 1. We can see that α increases with the decreased compliance current because of the different interface states.

4. Summary

In summary, reproducible RS in Ag/NiO/NSTO/In device has been investigated for nonvolatile memory application. By changing the max forward voltage and compliance current, the devices showed multilevel LRS, and by changing the reverse voltage, the device can obtain multilevel HRS. The retention characteristic exhibits nonvolatile nature. The origin of the RS behavior would be attributed to the carrier injection trapped/detrapped at the interface of the heterojunction. The whole resistance of the device includes the interface barrier and the NiO films, but which one contributes larger? This is a question to separate contributions between interface barrier and real NiO films.

Acknowledgment

This work was supported by the National Natural Science Foundation of China (Grant no. 11074193 and no. 51132001).

References

[1] A. Sawa, "Resistive switching in transition metal oxides," *Materials Today*, vol. 11, no. 6, pp. 28–36, 2008.

[2] R. Waser, R. Dittmann, C. Staikov, and K. Szot, "Redox-based resistive switching memories nanoionic mechanisms, prospects, and challenges," *Advanced Materials*, vol. 21, no. 25-26, pp. 2632–2663, 2009.

[3] S. Seo, M. J. Lee, D. H. Seo et al., "Reproducible resistance switching in polycrystalline NiO films," *Applied Physics Letters*, vol. 85, no. 23, pp. 5655–5657, 2004.

[4] M. Kawai, K. Ito, and Y. Shimakawa, "Resistance switching in a single-crystalline NiO thin film grown on a $Pt_{0.8}Ir_{0.2}$ electrode," *Applied Physics Letters*, vol. 95, no. 1, Article ID 012109, 3 pages, 2009.

[5] J. S. Choi, J. S. Kim, I. R. Hwang et al., "Different resistance switching behaviors of NiO thin films deposited on Pt and $SrRuO_3$ electrodes," *Applied Physics Letters*, vol. 95, no. 2, Article ID 022109, 3 pages, 2009.

[6] F. Kurnia, H. Hadiyawarman, C. U. Jung et al., "Effect of NiO growth conditions on the bipolar resistance memory switching of Pt/NiO/SRO structure," *Journal of the Korean Physical Society*, vol. 57, no. 61, pp. 1856–1861, 2010.

[7] S. H. Chang, J. S. Lee, S. C. Chae et al., "Occurrence of both unipolar memory and threshold resistance switching in a NiO film," *Physical Review Letters*, vol. 102, no. 2, Article ID 026801, 4 pages, 2009.

[8] C. B. Lee, B. S. Kang, A. Benayad et al., "Effects of metal electrodes on the resistive memory switching property of NiO thin films," *Applied Physics Letters*, vol. 93, no. 4, Article ID 042115, 3 pages, 2008.

[9] S. H. Phark, R. Jung, Y. J. Chang, T. W. Noh, and D. W. Kim, "Interfacial reactions and resistive switching behaviors of metal/NiO/metal structures," *Applied Physics Letters*, vol. 94, no. 2, Article ID 022906, 3 pages, 2009.

[10] J. Sullaphen, K. Bogle, X. Cheng et al., "Interface mediated resistive switching in epitaxial NiO nanostructures," *Applied Physics Letters*, vol. 100, no. 20, Article ID 203115, 5 pages, 2012.

[11] S. X. Wu, L. M. Xu, X. J. Xing et al., "Reverse-bias-induced bipolar resistance switching in $PtTiO_2$ $SrTi_{0.99}Nb_{0.01}O_3$/Pt devices," *Applied Physics Letters*, vol. 93, no. 4, Article ID 043502, 3 pages, 2008.

[12] S. X. Wu, H. Y. Peng, and T. Wu, "Concurrent nonvolatile resistance and capacitance switching in $LaAlO_3$," *Applied Physics Letters*, vol. 98, no. 9, Article ID 093503, 3 pages, 2011.

[13] J. J. Yang, M. D. Pickett, X. Li, D. A. A. Ohlberg, D. R. Stewart, and R. S. Williams, "Memristive switching mechanism for metal/oxide/metal nanodevices," *Nature Nanotechnology*, vol. 3, no. 7, pp. 429–433, 2008.

[14] H. Y. Peng, G. P. Li, J. Y. Ye et al., "Electrode dependence of resistive switching in Mn-doped ZnO: filamentary versus interfacial mechanisms," *Applied Physics Letters*, vol. 96, no. 19, Article ID 192113, 3 pages, 2010.

[15] M. C. Wu, Y. W. Lin, W. Y. Jang, C. H. Lin, and T. Y. Tseng, "Low-power and highly reliable multilevel operation in ZrO2 1T1R RRAM," *IEEE Electron Device Letters*, vol. 32, no. 8, pp. 1026–1028, 2011.

[16] S. L. Li, D. S. Shang, J. Li, J. L. Gang, and D. N. Zheng, "Resistive switching properties in oxygen-deficient $Pr_{0.7}Ca_{0.3}MnO_3$ junctions with active Al top electrodes," *Journal of Applied Physics*, vol. 105, no. 3, Article ID 033710, 2009.

[17] M. C. Ni, S. M. Guo, H. F. Tian et al., "Resistive switching effect in $SrTiO_{3-\delta}$/Nb-doped $SrTiO_3$ heterojunction," *Applied Physics Letters*, vol. 91, no. 18, Article ID 183502, 3 pages, 2007.

[18] M. H. Lin, M. C. Wu, C. H. Lin, and T. Y. Tseng, "Resistive switching characteristics and mechanisms of Pt-embedded $SrZrO_3$ memory devices," *Journal of Applied Physics*, vol. 107, no. 12, Article ID 124117, 4 pages, 2010.

[19] H. F. Tian, Y. G. Zhao, X. L. Jiang, J. P. Shi, H. J. Zhang, and J. R. Sun, "Resistance switching effect in LaAlO3/Nb-doped $SrTiO_3$ heterostructure," *Applied Physics A*, vol. 102, no. 4, pp. 939–942, 2011.

[20] Y. Chen, L. Chen, G. Lian, and G. Xiong, "Resistance and superconductivity switching caused by carrier injection: evidences of self-trapping carriers in oxide electronics," *Journal of Applied Physics*, vol. 106, no. 2, Article ID 023708, 7 pages, 2009.

[21] Y. S. Chen, L. P. Chen, G. J. Lian, and G. C. Xiong, "Resistance switching characteristic and charge carrier self-trapping in epitaxial $Pr_{0.7}(Ca_{1-x}Sr_x)_{0.3}MnO_3$ thin films," *Chinese Physics Letters*, vol. 26, no. 3, Article ID 037201, 2009.

[22] S. E. Savel'ev, A. S. Alexandrov, A. M. Bratkovsky, and R. S. Williams, "Molecular dynamics simulations of oxide memristors: thermal effects," *Applied Physics A*, vol. 102, no. 4, pp. 891–895, 2011.

[23] S. E. Savel'ev, A. S. Alexandrov, A. M. Bratkovsky et al., "Molecular dynamics simulations of oxide memristors: crystal field effects," *Applied Physics Letters*, vol. 99, no. 5, Article ID 053108, 3 pages, 2011.

[24] S. E. Savel'Ev, A. S. Alexandrov, A. M. Bratkovsky, and R. Stanley Williams, "Molecular dynamics simulations of oxide memory resistors (memristors)," *Nanotechnology*, vol. 22, no. 25, Article ID 254011, 2011.

[25] D. S. Jeong, R. Thomas, R. S. Katiyar et al., "Emerging memories: resistive switching mechanisms and current status," *Reports on Progress in Physics*, vol. 75, no. 7, Article ID 076502, 2012.

[26] H. Shima, F. Takano, H. Akinaga, Y. Tamai, I. H. Inoue, and H. Takagi, "Resistance switching in the metal deficient-type oxides: NiO and CoO," *Applied Physics Letters*, vol. 91, no. 1, Article ID 012901, p. 3, 2007.

[27] Y. S. Chen, B. Chen, B. Gao et al., "Anticrosstalk characteristics correlated with the set process for α -Fe_2O_3/Nb- $SrTiO_3$ stack-based resistive switching device," *Applied Physics Letters*, vol. 97, no. 26, Article ID 262112, 3 pages, 2010.

[28] X. T. Zhang, Q. X. Yu, Y. P. Yao et al., "Ultrafast resistive switching in $SrTiO_3$:Nb single crystal," *Applied Physics Letters*, vol. 97, no. 22, Article ID 222117, 3 pages, 2010.